UNIVERSIDAD TÉCNICA DE MANABÍ
Fundada en 1952

BASES DE LA CIENCIA
REVISTA CIENTÍFICA
FACULTAD DE CIENCIAS BÁSICAS
Portoviejo - Manabí - Ecuador

Ciencias Químicas

PHOTOELECTROCHEMICAL DEGRADATION OF IMATINIB MESYLATE USING A BDD/TIO_2 PHOTOANODE: A SHORT COMMUNICATION

DEGRADACIÓN FOTOELECTROQUÍMICA DE MESILATO DE IMATINIB UTILIZANDO UN FOTOÁNODO BDD/TIO_2: UNA COMUNICACIÓN CORTA

DEGRADACAO FOTOELETROQUIMICA DO MESILATO DE IMATINIB UTILIZANDO UM FOTOÂNODO BDD/TIO_2: UMA COMUNICACAO CURTA

Autores:

Steven Mateo Vélez Zambrano[1,2]
svelez6538@utm.edu.ec

G. Xavier Castillo-Cabrera[1]
GXCASTILLO@puce.edu.ec

Gustavo Altamirano-Briones[2,3]
gustavo.altamirano@alu.uhu.es

Patricio Javier Espinoza-Montero[1,*]
pespinoza646@puce.edu.ec

[1]Pontificia Universidad Católica de Ecuador, Quito, Ecuador

[2]Universidad Técnica de Manabí, Portoviejo, Ecuador

[3]Programa de Doctorado en Ciencia y Tecnología Industrial y Ambiental, Universidad Huelva, Huelva, España

* Autor para correspondencia.

Editor Académico
Jesús Ágreda

Citación sugerida: Velez Zambrano, S.M., Castillo Cabrera, G.X., Altamirano-Briones, G., Espinoza-Montero, P.J. (2025). Photoelectrochemical degradation of imatinib mesylate using a BDD/TiO_2 photoanode: A short communication. *Revista Bases de la Ciencia, 10(3)*, 30-43. DOI: 10.33936/revbasdelaciencia.v10i3.7677

Recibido: 28/06/2025
Aceptado: 17/11/2025
Publicado: 17/12/2025

Abstract

Imatinib (IMB) is an enzymatic inhibitor that prevents the proliferation of cancer cells. It is used to treat certain types of cancer, such as leukemia, and is also effective in the treatment of specific gastrointestinal stromal tumors and dermatofibrosarcoma protuberans. After administration, it is excreted through urine and feces. The concentration of IMB in the environment is increasing rapidly, leading to serious environmental and human health concerns. This study employs a boron-doped diamond photoanode modified with titanium dioxide (BDD/TiO_2) for the degradation of IMB via photoelectrocatalysis. The research was divided into three stages: i) modification of the BDD electrode through electrophoretic deposition of synthetic TiO_2 nanoparticles; ii) electrochemical characterization of the BDD/TiO_2 photoanode; iii) degradation of imatinib (24 mg L^{-1}) through electrochemical oxidation using BDD and photoelectrocatalysis with BDD/TiO_2 at various current densities over 90 minutes. Degradation and mineralization were monitored using UV spectroscopy and chemical oxygen demand (COD) analysis. The highest photoelectrocatalytic degradation rate of IMB reached 84.09 % when applying a current density of 8.26 mA cm^{-2}.

Keywords: Imatinib mesylate (IMB), Photoelectrocatalysis (PEC), Photoanode, Electrophoretic deposition, Boron Doped Diamond (BDD), Titanium Dioxide (TiO_2).

Resumen

El imatinib (IMB) es un inhibidor enzimático que previene la propagación de las células cancerosas. Se utiliza para tratar ciertos tipos de cáncer, como la leucemia. También es útil para el tratamiento de ciertos tipos de tumores del estroma gastrointestinal y del dermatofibrosarcoma protuberante. Tras su consumo, se elimina mediante la orina y materia fecal. La cantidad de IMB en el ambiente está creciendo rápidamente, causando serios problemas ambientales y en la salud humana. Este estudio utiliza un fotoánodo de Diamante Dopado con Boro modificado con Dióxido de Titanio (BDD/TiO_2) para la degradación de IMB mediante fotoelectrocatálisis. El estudio se dividió en tres etapas: i) modificación del BDD mediante deposición electroforética de nanopartículas sintéticas de TiO_2; ii) caracterización electroquímica del fotoánodo BDD/TiO_2; iii) degradación de imatinib (24 mg L^{-1}) mediante oxidación electroquímica con BDD y fotoelectrocatálisis sobre BDD/TiO_2 a diferentes densidades de corriente durante 90 min. La degradación y mineralización se monitorearon mediante espectroscopia UV y demanda química de oxígeno. La tasa máxima de degradación fotoelectrocatalítica del IMB fue del 84.09 %, aplicando una densidad de corriente de 8.26 mA cm^{-2}.

Palabras clave: Mesilato de imatinib (IMB), Fotoelectrocatálisis (FEC), Fotoánodo, Depósito electroforético, Diamante Dopado con Boro (BDD), Dióxido de Titanio (TiO_2).

Resumo

O imatinibe (IMB) é um inibidor enzimático que impede a proliferação de células cancerígenas. É utilizado no tratamento de certos tipos de câncer, como a leucemia. Também é eficaz no tratamento de determinados tipos de tumores do estroma gastrointestinal (GIST) e do dermatofibrossarcoma protuberante. Após sua administração, é eliminado por meio da urina e das fezes. A concentração de IMB no ambiente está aumentando rapidamente, causando sérios problemas ambientais e riscos à saúde humana. Este estudo utiliza um fotoânodo de diamante dopado com boro, modificado com dióxido de titânio (BDD/TiO_2), para a degradação do IMB por meio da fotoeletrocatálise. A pesquisa foi dividida em três etapas: i) modificação do eletrodo BDD por deposição eletroforética de nanopartículas sintéticas de TiO_2; ii) caracterização eletroquímica do fotoânodo BDD/TiO_2; iii) degradação do imatinibe (24 mg L^{-1}) por oxidação eletroquímica com BDD e fotoeletrocatálise com BDD/TiO_2 sob diferentes densidades de corrente durante 90 minutos. A degradação e a mineralização foram monitoradas por espectroscopia UV e pela análise de demanda química de oxigênio (DQO). A taxa máxima de degradação fotoeletrocatalítica do IMB foi de 84.09 %, aplicando uma densidade de corrente de 8.26 mA cm^{-2}.

Palavras chave: Mesilato de imatinibe (IMB), Fotoeletrocatálise (FEC), Fotoânodo, Deposição eletroforética, Diamante dopado com boro (BDD), dióxido de tiânio (TiO_2).

UNIVERSIDAD TÉCNICA DE MANABÍ
Fundada en 1952

BASES DE LA CIENCIA
REVISTA CIENTÍFICA
FACULTAD DE CIENCIAS BÁSICAS
Portoviejo - Manabí - Ecuador

1. Introduction

The large-scale production and consumption of pharmaceutical compounds have become a major environmental concern, as most of these substances ultimately reach and contaminate natural water sources (Vasilachi et al., 2021). Although their residual concentrations are typically low, many pharmaceuticals can bioaccumulate and enter the trophic chain, leading to long-term adverse effects on plants, animals, and human health (Gondi et al., 2022).

Cytostatic drugs (CDs) are classified as contaminants of emerging concern (CECs) because they are not currently regulated, despite their well-documented toxicological and ecological impacts (Domingo-Echaburu et al., 2022). Among these compounds, imatinib mesylate ($C_{29}H_{31}N_7O \cdot CH_3SO_3H$; IMB) stands out as the first clinically approved protein kinase inhibitor used in cancer therapy. Unlike most CDs, IMB does not interact directly with DNA, offering a more selective and promising therapeutic approach. As a result, its global consumption has increased exponentially (Novak et al., 2017). IMB exhibits high bioavailability (approximately 98 %) and is primarily excreted through feces (68 %) and, to a lesser extent, urine (13 %) (Serna Siatova & Cárdenas Losada, 2018).

Environmental studies have revealed growing concern regarding the persistence of IMB in aquatic ecosystems. Novak et al. (2017) reported IMB concentrations in European water bodies ranging between 3.3 and 5.0 ng L^{-1}, levels initially considered below ecotoxic thresholds. However, subsequent monitoring by the same group in 2021 revealed an increase to 13 ng L^{-1}, more than doubling the previous concentrations and highlighting the escalating issue of pharmaceutical residues in the environment (Novak et al., 2021). In toxicological studies, IMB exposure was shown to induce mutagenic effects in mice, including hyperplasia of the interstitial cells of Cajal and retention of intestinal contents in the caecum (Klein-Rodewald et al., 2022).

The continuous rise of IMB contamination underscores the urgent need for effective and sustainable treatment strategies. In this context, advanced oxidation processes (AOPs) have emerged as promising technologies for degrading persistent and complex pollutants such as CECs (Mishra et al., 2023). Among AOPs, photoelectrocatalysis (PEC) has attracted particular attention due to its high efficiency, environmental compatibility, and ability to mineralize recalcitrant organic contaminants.

PEC operates through a three-step mechanism: (i) a photocatalyst deposited on a conductive substrate (photoelectrode) absorbs incident photons, promoting electrons from the valence band (VB) to the conduction band (CB) and generating electron–hole pairs; (ii) an external bias potential is applied to extract photogenerated carriers, thereby enhancing charge separation and minimizing recombination; and (iii) the resulting holes (h+) in the VB drive oxidation reactions, ideally producing hydroxyl radicals $\cdot OH$ from water, which can non-selectively oxidize organic pollutants (Espinoza-Montero et al., 2022). The application of an external potential in PEC systems provides a significant advantage over conventional photocatalysis, as it increases the lifetime and reactivity of charge carriers, thus improving overall oxidation efficiency.

The degradation efficiency of organic pollutants is strongly influenced by the type of photocatalyst used as photoanode (Alulema-Pullupaxi et al., 2021). According to Espinoza-Montero et al., (2022), the selection of photoanode materials determines the properties of the photoelectrode and the overall degradation performance. In the case of boron-doped diamond substrates (BDD), the introduction of boron atoms creates electron deficiencies (positive holes) in the crystal lattice. In the band structure, the Fermi level is closer to the valence band (VB), and when electrons are stimulated by light (or the application of potential), they move from the VB to the conducting band (CB).

In this case, there are more holes in the VB than electrons in the CB, so the BDD exhibits p-type semiconductor behavior (Rycewicz et al., 2022; Sultana et al., 2025). In contrast, the presence of oxygen vacancies in TiO_2 introduces a pair of electrons into the lattice. When light is applied, these electrons are excited from VB to CB (Asadollahi et al., 2020; Kayani et al., 2023; Zhu et al., 2022). Under these conditions, TiO_2 has a greater number of free electrons than holes and exhibits n-type semiconductor behaviour. The p–n heterojunction formed between BDD and TiO_2 facilitates efficient charges separation and transport, improving the photoelectrocatalytic performance.

On the other hand, BDD/TiO_2 photoanodes combine efficiency and environmental safety. BDD is chemically inert, electrochemically stable, and does not evict harmful species, while TiO_2 is biocompatible and widely recognized as a non-toxic photocatalyst (Terashima et al., 2016). In addition, BDD/TiO_2 is a p-n heterojunction which offers clear functional advantages: (i) efficient charge carriers separation, (ii) higher electrical conductivity that reduces the loss of recombination, (iii) synergy between electrooxidation in BDD and photocatalysis in TiO_2, and (iv) long-term mechanical and chemical stability.

Several strategies have been explored to mitigate the environmental impact of cancer drugs, particularly through their degradation using light driven technologies such as photocatalysis and PEC. Mazierski et al., (2023) used a

CdS/TiO_2 photoanode to degrade ifosfamide, 5-fluorouracil, and imatinib mesylate in three-hour reactions, achieving a TOC elimination of 48 ± 2.4 %, 40 ± 2.2 %, and 24 ± 1.8 %, respectively. Although effective, CdS poses a critical drawback: cadmium is a highly toxic heavy metal, and despite controls to detect leaching, its potential release and the photocorrosion of CdS significantly limit long-term applicability (Wei et al., 2021). Similarly, Naraginti et al., (2019) reported 90 % degradation of azithromycin using a ZrO_2/Ag@TiO_2 photoanode under visible light. However, the incorporation of silver also raises concerns about cost and ecotoxicity due to potential metal release.

BDD/TiO_2 composites are among the most robust and widely studied photoelectrodes for this purpose and have shown excellent performance in reducing complex and persistent organic compounds in water environments, including glyphosate (Alulema-Pullupaxi et al., 2021), diclofenac (Sigcha-Pallo et al., 2022), and microplastics (Quilumbaquin, Castillo-Cabrera, Borrero-González, Mora et al., 2024). This photoanode exhibits high long-term stability, efficient photoelectrochemical activity, and environmental safety, since TiO_2 is non-toxic and biocompatible (Jerczynski et al., 2022).

In this study, we utilized the BDD/TiO_2 photoanode to evaluate its efficiency in the degradation of IMB by PEC. Additionally, we explored the optimal operating conditions for this system, providing a foundation for further research aimed at improving both the photoanode material and operational parameters.

2. Materials and Methods

Reagents

All reagents were used without further purification. Sodium sulfate (Sigma Aldrich, CAS 7757-82-6, reagent grade), sulfuric acid (Sigma Aldrich, CAS 7664-93-9, 98 %), potassium ferricyanide (Sigma Aldrich, CAS 13746-66-2, 98 %), imatinib mesylate (Anhui Haikang Pharmaceutical, CAS 220127-57-1), potassium ferrocyanide (Sigma Aldrich, CAS 14459-95-1, 98 %), BDD/Nb (Metakem™, Germany; geometric area = 8.5 cm^2), Degussa P25 titanium dioxide nanopowder (Sigma Aldrich, CAS 13463-67-7), perchloric acid (Sigma Aldrich, 98 %), and COD LR reagent vials (Hanna Instruments) were used in this study.

Equipment

For electrochemical and photoelectrochemical measurements, a CH Instruments 1230 electrochemical workstation was used. PEC experiments were conducted using a UV LED lamp (Cole-Parmer, T8 20 W, 110 V, 245 nm) as the light source and an AC/DC power supply (BK Precision, 1760A) for degradation. IMB degradation was monitored using the HACH COD test (HACH 8000, Usepa HAC-H-2000) and a UV–Vis spectrometer (Agilent Technologies, Cary 60).

Methods

Prior to modification, the boron-doped diamond (BDD) electrode was electrochemically activated and subsequently coated with TiO_2 via electrophoretic deposition, following the procedure previously described by our group (Quilumbaquin, Castillo-Cabrera, Borrero-González & Espinoza-Montero, 2024). Briefly, a 2.5 % (w/v) TiO_2 suspension was prepared in a 2.5 % (v/v) isopropyl alcohol–water solvent mixture, with a total volume of 25 mL.

An electrochemical cell was then assembled, consisting of the BDD electrode as the working electrode and an aluminum plate as the counter electrode. Both electrodes were immersed in the TiO_2 suspension for 15 s under an applied potential of 4.8 V. Following deposition, the modified electrode was dried on a hot plate at 100 °C for 5 min and subsequently subjected to thermal treatment in an oven at 200 °C for 20 min to ensure proper adhesion and crystallization of the TiO_2 layer.

a) Characterization

For electrochemical and photoelectrochemical characterizations, a three-electrode system was employed, consisting of either bare BDD or BDD/TiO_2 as the working electrode, a platinum mesh as the counter electrode, and an Ag/AgCl reference electrode, all enclosed within a Faraday cage to minimize electronic noise. To evaluate the enhancement in

UNIVERSIDAD TÉCNICA DE MANABÍ
Fundada en 1952

BASES DE LA CIENCIA
REVISTA CIENTÍFICA
FACULTAD DE CIENCIAS BÁSICAS
Portoviejo - Manabí - Ecuador

active surface area and photoactivity upon TiO_2 modification, CV experiments were performed using a 2 mmol L^{-1} ferricyanide redox couple in 1 mol L^{-1} KCl under both UV-illuminated and dark conditions.

In order to determine the working potential window of the electrodes and select the appropriate potentials for transient photocurrent experiments, CV was performed in 0.1 mol L^{-1} sodium sulfate solution. Light-chopped photocurrent experiments (transient photocurrent) were then conducted at the previously determined potentials according to the CV profiles, using only the electrolyte solution to assess the photocurrent generated by the photocatalyst layer. The experiments were carried out in a transient mode, consisting of 5 minutes of dark pre-conditioning for stabilization, followed by 2 minutes of light activation, 10 seconds of photocurrent recording, and 4 minutes for the system to return to the ground state, with a total of 10 cycles of measurement.

b) Degradation of IMB

The degradation of imatinib mesylate (IMB) was monitored using UV–Vis spectroscopy at 257 nm (Bende et al., 2008) with an integration time of 12.5 ms. A calibration curve was constructed using IMB standard solutions at concentrations of 1, 5, 10, 20, 30, 40, and 50 μmol L^{-1} prepared in 0.1 mol L^{-1} sodium sulfate, which served as the supporting electrolyte.

Both electrocatalytic (EC) and photoelectrocatalytic (PEC) degradation processes were evaluated. Experiments were conducted using 35 mL of a 24 mg L^{-1} IMB solution in 0.1 mol L^{-1} Na_2SO_4 under continuous magnetic stirring, for reaction times of 10, 20, 30, 60, and 90 min. UV irradiation (4 mW cm^{-2}) was supplied by two LED emitters, and the applied current density was varied between 4.13, 8.26, and 11.35 mA cm^{-2}. To prevent temperature fluctuations from affecting hydroxyl radical ($^{\bullet}OH$) generation, two cooling gels were positioned on either side of the electrochemical cell.

A platinum mesh was used as the counter electrode, while an Ag/AgCl electrode served as the reference to maintain control of the anodic potential during degradation. Electrooxidation (EO) experiments were carried out under identical conditions but without UV illumination, employing either a bare BDD anode or a TiO_2-modified BDD (BDD/TiO_2) anode for comparative evaluation.

The degradation process was monitored by UV–Vis spectroscopy at a fixed wavelength of 257 nm. After each degradation experiment, performed at the specified time intervals, aliquots of the treated solution were collected and preserved with concentrated sulfuric acid for subsequent chemical oxygen demand (COD) analysis using the HACH 8000 test system. All experiments were conducted in triplicate to ensure statistical reliability.

The specific energy consumption (EC) of the PEC process was calculated according to the following equation (Castillo-Cabrera et al., 2023):

$$\text{E.C}\ (\text{kWh}\,\text{m}^{-3}) = \frac{E_{\text{cell}} \cdot I \cdot t}{V_s} \tag{1}$$

Where E_{cell} is the applied cell potential (V), I is the current passing through the cell (A), t is the reaction time (h), and V_s is the solution volume (m^3).

The operating cost of the process was calculated (Castillo-Cabrera et al., 2023):

$$\text{Cost of process} = \text{E.C}\ (\text{kWh}\,\text{m}^{-3}) \cdot \text{Unit electricity price}\ (\text{USD}\,\text{kWh}^{-1}) \tag{2}$$

3. Results and Discussion

Figure 1a presents the cyclic voltammetry (CV) profiles obtained for the ferri/ferrocyanide redox couple. The BDD/TiO_2 electrode exhibits higher anodic and cathodic peak current densities than the bare BDD electrode, indicating an enhancement of the electroactive surface area due to the deposition of the TiO_2 photocatalyst layer.

Figure 1b shows the voltammetric response recorded in 0.1 mol L^{-1} Na_2SO_4, revealing distinct differences in oxidation and reduction overpotentials between the two electrodes. These variations suggest improved electrocatalytic performance of the BDD/TiO_2 photoelectrode. The observed increase in capacitive current within the potential range of -0.5 to -1.25 V is characteristic of the charging and discharging processes associated with electrodes modified by semiconductor materials.

revista.bdlaciencia@utm.edu.ec | Vol. 10. Núm. 3 (30-43): septiembre-diciembre, 2025 | DOI: 10.33936/revbasdelaciencia.v10i3.7677

Upon UV illumination, the BDD/TiO_2 electrode displays a clear decrease in oxidation overpotential (Figure 1c), confirming the photoactivation of the TiO_2 layer and its contribution to the overall photocatalytic behavior of the composite electrode.

Figure 1d illustrates the transient photocurrent responses recorded at applied potentials of 1.50, 1.55, and 1.60 V *vs.* Ag/AgCl. At 1.50 V, the photocurrent increases from a baseline of 0.003 to 0.006 μA cm^{-2}; at 1.55 V, from 0.007 to 0.012 μA cm^{-2}; and at 1.60 V, from 0.016 to 0.027 μA cm^{-2}. The highest photocurrent response was observed at 1.60 V, corresponding to a net increase of 0.011 μA cm^{-2}. These results indicate that higher applied potentials promote more efficient charge separation and enhanced photoelectrocatalytic activity of the BDD/TiO_2 electrode.

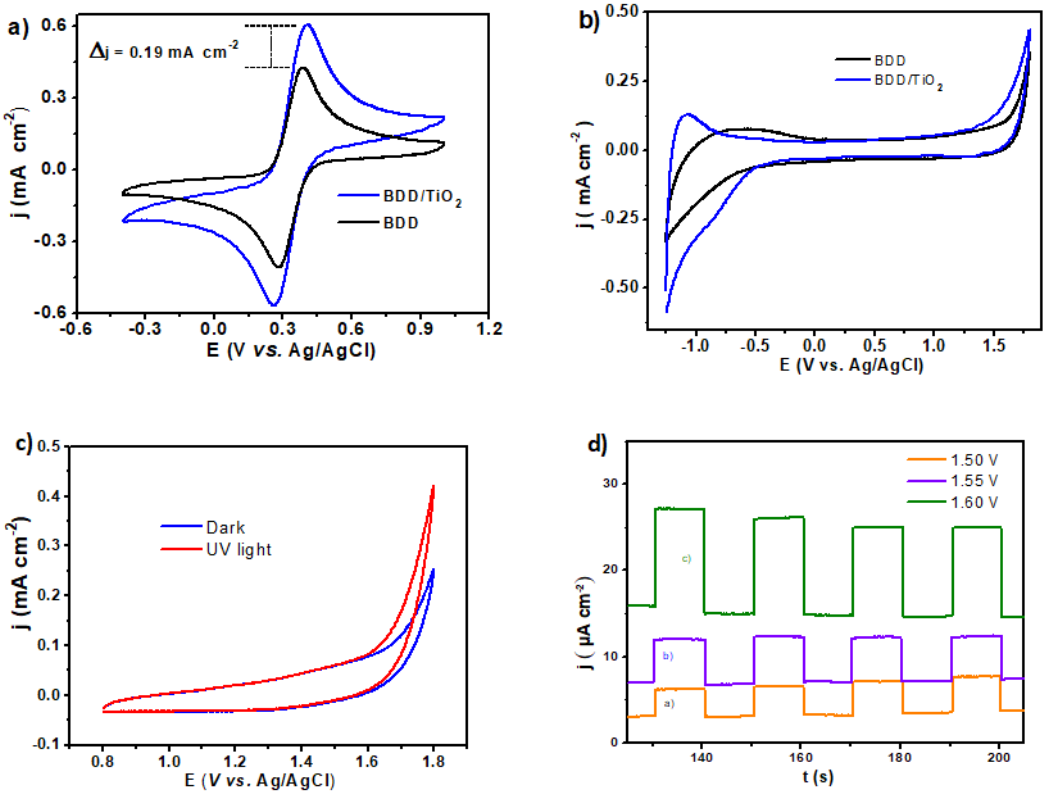

Figure 1. Electrochemical and photoelectrochemical characterization of BDD and BDD/TiO_2 electrodes. **a)** CV profiles of BDD and BDD/TiO_2 in 2.0 mmol L^{-1} $[Fe(CN)_6]^{3-/4-}$ redox couple in 1.0 mol L^{-1} KCl. **b)** CV profiles of BDD and BDD/TiO_2 in 0.1 mol L^{-1} Na_2SO_4. **c)** CV profiles of BDD/TiO_2 in 0.1 mol L^{-1} Na_2SO_4 under dark and UV illumination conditions. **d)** Transient photocurrent response of BDD/TiO_2 in 0.1 mol L^{-1} Na_2SO_4 under chopped UV light.

Photoelectrocatalytic Degradation of IMB

Three distinct current densities, 4.13, 8.26, and 11.35 mA cm^{-2}, were evaluated for the electrochemical and photoelectrochemical oxidation of IMB. These values were selected based on $^{\bullet}$OH-radical scavenging experiments conducted by (Quilumbaquin, Castillo-Cabrera, Borrero-González, Mora et al., 2024), which identified the optimal range for generating oxidant species under the specific photoanode material and cell conditions.

Figure 2a presents the degradation percentages of IMB over 90 min PEC reactions at different current densities. The results indicate that the degradation efficiencies at 8.26 and 11.35 mA cm^{-2} are statistically equivalent, achieving 84.09 % and 82.95 % respectively. In contrast, a lower efficiency of 62.14 % was observed at 4.13 mA cm^{-2}. These findings highlight that a current density of 8.26 mA cm^{-2} provides the highest degradation efficiency while minimizing energy consumption compared to the higher current density.

Similar trends were observed in the electrochemical oxidation of IMB using the bare BDD and the BDD/TiO_2 (Figure 1), confirming that the PEC process with the BDD/TiO_2 photoanode offers superior performance for IMB degradation

UNIVERSIDAD TÉCNICA DE MANABÍ
Fundada en 1952

BASES DE LA CIENCIA
REVISTA CIENTÍFICA
FACULTAD DE CIENCIAS BÁSICAS
Portoviejo - Manabí - Ecuador

under the conditions evaluated in this study.

Figure 1b presents the pseudo-first-order kinetic analysis for the PEC degradation of IMB at the tested current densities. The highest apparent rate constant was observed at 11.35 mA cm^{-2}, with a value of 0.0295 min^{-1}. However, the corresponding coefficient of determination (R^2) was relatively low, indicating poor linearity and limited statistical confidence in the fit—suggesting that side reactions or mass transport limitations may be influencing the degradation behavior at this higher current density. At 8.26 mA cm^{-2}, the apparent kinetic constant slightly decreased to 0.024 min^{-1}, yet the R^2 value improved significantly, indicating a better fit to the pseudo-first-order model and greater statistical reliability. This suggests a more controlled and efficient degradation process under these conditions. In contrast, the lowest current density (4.13 mA cm^{-2}) yielded the lowest rate constant, reflecting a slower degradation rate caused by limited generation of oxidant species or inefficient separation of charge carriers. A similar kinetic trend was observed in electrochemical oxidation experiments using both BDD and BDD/TiO_2 electrodes without photoactivation (Figure 1), reinforcing the observation that intermediate current density not only offers improved energy efficiency but also more predictable and reliable kinetic behavior in IMB degradation.

When comparing the degradation processes (PEC and EO) at a current density of 8.26 mA cm^{-2}, we find that the PEC process has a higher apparent kinetic constant, mainly due to the synergistic effect of the BDD/TiO_2 heterojunction and UV irradiation. As shown in Figure 3, the CB and VB positions of TiO_2 differ significantly from those of BD, favoring charge separation. By using a bias potential, holes from the BDD are injected into the VB of the TiO_2, while electrons from the TiO_2 are injected into the CB of the BDD, allowing for easy separation of charge carriers between the two materials. The band alignment at the BDD/TiO_2 interface facilitates charge transfer and suppresses recombination. The photogenerated h^+ in the VB, together with pre-existing oxygen vacancies in TiO_2, contribute to the generation of $^{\bullet}OH$, which play a key role in the enhanced degradation and mineralization of IMB. (Alulema-Pullupaxi et al., 2021; Castillo-Cabrera et al., 2023; Terashima et al., 2016; Xie et al., 2022).

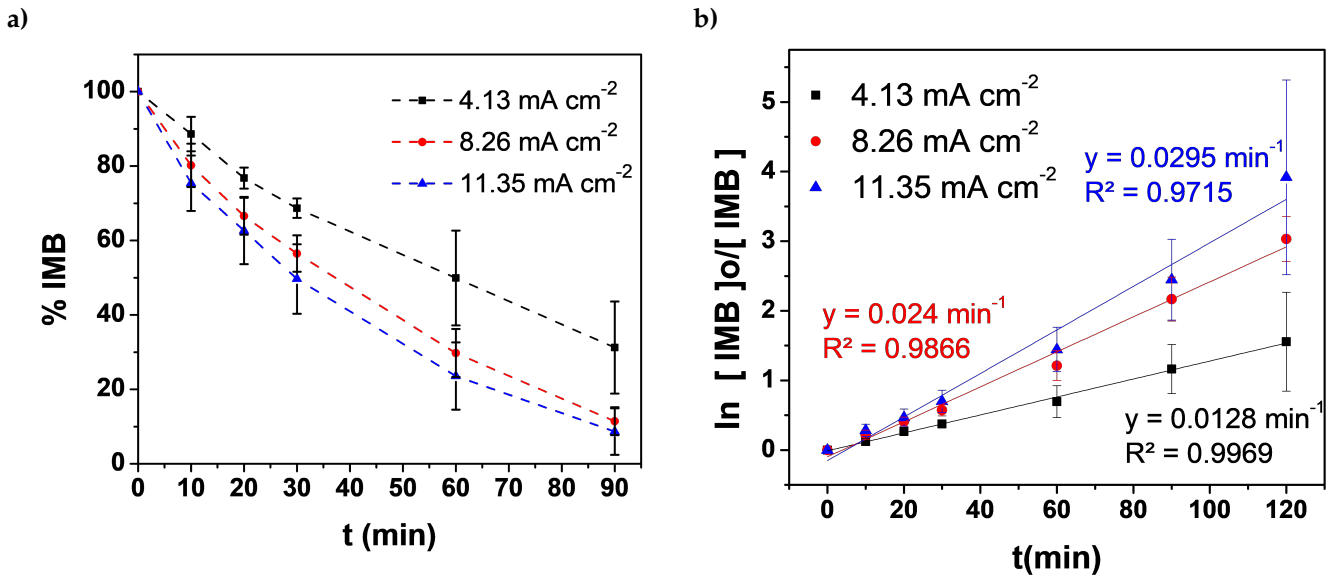

Figure 2. a) IMB degradation efficiency during 90 min of PEC reactions at different current densities (4.13, 8.26, and 11.35 mA cm^{-2}) in 0.1 mol L^{-1} Na_2SO_4. b) Pseudo-first-order kinetic analysis of the degradation process, showing the influence of current density on the apparent rate constant and the linear fit to the kinetic model. Data are presented as mean ± standard deviation, as detailed in Table 1.

revista.bdlaciencia@utm.edu.ec | Vol. 10. Núm. 3 (30-43): septiembre-diciembre, 2025 | DOI: 10.33936/revbasdelaciencia.v10i3.7677

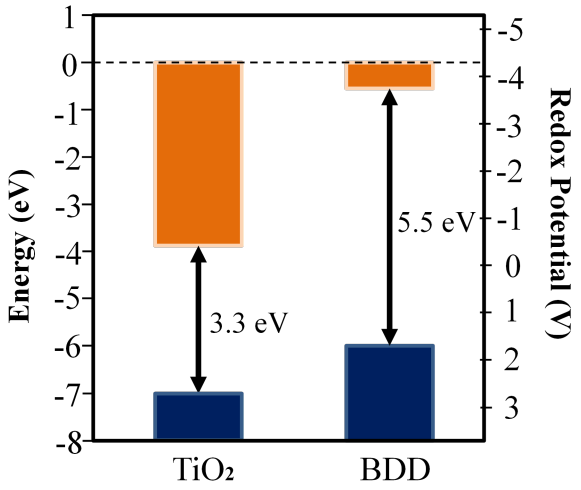

Figure 3. Electronic band positions of TiO_2 and BDD with respect to vacuum level and standard hydrogen electrode. Adapted from Terashima et al., (2016).

The chemical oxygen demand (COD) was measured to evaluate the mineralization efficiency of each process. Figure 4 presents the percentage of COD removal over time for the PEC system. After 90 min of reaction, the BDD/TiO_2 photoanode achieved a COD concentration of 12.16 mg L^{-1}, representing the lowest residual value among the tested systems. This result indicates a higher degree of IMB degradation compared to both EO using the same BDD/TiO_2 photoanode and the bare BDD electrode. The enhanced mineralization observed in the PEC system can be attributed to the synergistic effects of photogenerated electron-hole pairs due to the surface activity of the BDD/TiO_2 photoanode.

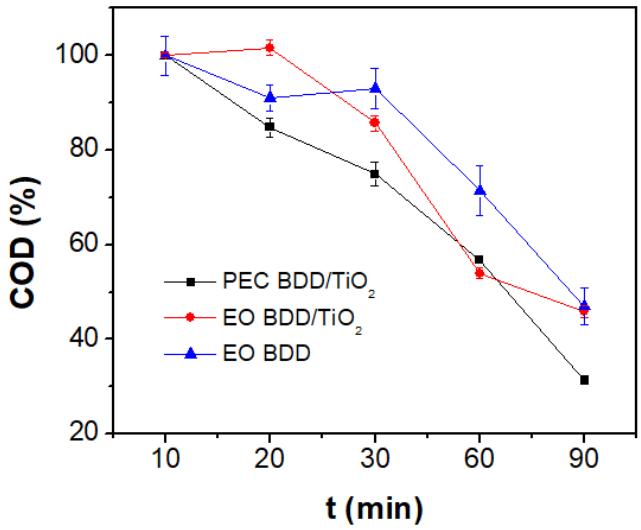

Figure 4. COD analysis for the degradation of IMB using PEC and EO with the bare BDD and BDD/TiO_2 anodes. (see Table 1).

For comparison, Table 1 presents the concentration of COD removal and the corresponding mineralization achieved by the oxidation processes evaluated. The PEC process exhibited a mineralization rate 14.57 % higher than obtained through EO using the BDD/TiO_2 photoanode. Similarly, the PEC system outperformed the EO process using the bare BDD anode, achieving a 15.66 % greater mineralization efficiency. These results demonstrate that the PEC process is the most effective technology for the degradation of IMB, highlighting its superior capability to promote almost complete oxidation of the pollutant compared to traditional electrochemical oxidation.

UNIVERSIDAD TÉCNICA DE MANABÍ
Fundada en 1952

BASES DE LA CIENCIA
REVISTA CIENTÍFICA
FACULTAD DE CIENCIAS BÁSICAS
Portoviejo - Manabí - Ecuador

Table 1. COD values and mineralization rates for IMB degradation after 90-min of reaction using PEC and EO processes.

Process	Electrode	COD (mg L^{-1})	Mineralization (%)
PEC	BDD/TiO_2	12.16	68.70
EO	BDD/TiO_2	13.6	54.13
EO	BDD	17	53.04

It is essential to develop cost-effective and energy-efficient strategies for the degradation of anticancer drugs to ensure their long-term environmental applicability. In Ecuador, the electricity cost is reported to be USD 0.095 per kWh as of December 2024 (Global Petrol Prices, 2024). Based on this rate, the operational cost of the proposed process is estimated at USD 0.91 per m^3 of treated solution. These findings demonstrate that the PEC process can achieve high degradation efficiency for complex oncological compounds while maintaining relatively low energy requirements.

In a related study, Sigcha-Pallo et al., (2022) reported the degradation of diclofenac sodium via PEC using a BDD/TiO_2 photoanode fabricated by electrophoretic deposition, achieving 98.5 % mineralization within two hours. The authors concluded that PEC systems exhibit lower energy consumption than electrooxidation (EO) processes, primarily due to the enhanced charge separation enabled by the p–n heterojunction. A similar trend was observed in the present work: during IMB degradation, the BDD/TiO_2 photoanode demonstrated reduced energy consumption under PEC conditions compared with EO operation.

Alulema-Pullupaxi et al., (2021) also employed PEC technology to degrade glyphosate using a TiO_2/BDD photoanode prepared via a sol–gel/spin-coating method with titanium oxysulfate as the precursor. Their process achieved 91.1 % glyphosate degradation with an energy consumption of 0.62 kWh $gTOC^{-1}$ over five hours, treating 400 mL of a 50 mg L^{-1} solution. In contrast, the present study achieved substantial degradation of the more complex IMB molecule in only 90 minutes, suggesting a lower energy demand per unit time. Nonetheless, the difference in solution volume–11.5 times smaller in this work–may partly explain the faster degradation kinetics observed.

For comparison, (Yang et al., 2019) reported complete mineralization of IMB via the electro-Fenton process using a graphene-modified carbon felt cathode (EEGr–CF), with an energy consumption (EC) of 14.4 kWh g^{-1}. In contrast, a conventional carbon felt cathode required 16.6 kWh g^{-1} under similar conditions. Although effective, the electro-Fenton process demanded higher current densities (16.66 mA cm^{-2}), longer reaction times (8 h), and larger solution volumes (150 mL). By comparison, the PEC process developed in this study achieved comparable mineralization efficiency at a lower current density (8.26 mA cm^{-2}) and significantly shorter reaction time (90 min), underscoring its superior energy efficiency.

Overall, when compared to other advanced oxidation processes, the proposed PEC system exhibits competitive advantages in terms of degradation efficiency, energy economy, and operational simplicity, positioning it as a promising technology for the sustainable treatment of pharmaceutical contaminants.

4. Conclusion

The BDD/TiO_2 photoanode demonstrated the highest efficiency among the tested oxidation systems, achieving 84.10 % degradation and 68.70 % mineralization of imatinib within 90 min under UV-assisted PEC conditions at an optimal current density of 8.26 mA cm^{-2}.

The TiO_2 coating effectively enhanced the surface properties of the BDD electrode, exhibiting sustained catalytic activity and mechanical integrity over prolonged operation (up to 7 h) without evidence of delamination or material degradation, confirming its durability for extended PEC applications.

Consistent with prior studies, the BDD/TiO_2 PEC system exhibited lower specific energy consumption compared to conventional electrooxidation, attributed to improved charge separation within the p–n heterojunction. However, optimization of light utilization and reactor configuration remains essential to further reduce energy costs and enable practical implementation in large-scale wastewater treatment.

revista.bdlaciencia@utm.edu.ec | Vol. 10. Núm. 3 (30-43): septiembre-diciembre, 2025 | DOI: 10.33936/revbasdelaciencia.v10i3.7677

5. Acknowledgments

The authors thank Pontificia Universidad Católica del Ecuador for funding through project Preparation of boron-doped diamond (BDD) photoelectrodes modified with bismuth semiconductors and their application in photoelectrocatalysis, code: QINV0402-IINV529020100, and Universidad Técnica de Manabí for financial support.

6. Conflict of Interest

The authors report no conflicts of interest related to this research.

7. References

Alulema-Pullupaxi, P., Fernández, L., Debut, A., Santacruz, C. P., Villacis, W., Fierro, C., & Espinoza-Montero, P. J. (2021). Photoelectrocatalytic degradation of glyphosate on titanium dioxide synthesized by sol-gel/spin-coating on boron doped diamond (TiO2/BDD) as a photoanode. *Chemosphere*, *278*, 130488. https://doi.org/10.1016/j.chemosphere.2021.130488

Asadollahi, E., Youzbashi, A. A., Keyanpour-Rad, M., & Eshraghi, M. J. (2020). Fabrication and investigation of optical and optoelectrical properties of phenyltriethoxysilane-capped TiO2 nanoparticle/poly(N-vinylcarbazol) hybrids. *Journal of Physics and Chemistry of Solids*, *136*, 109171. https://doi.org/10.1016/J.JPCS.2019.109171

Bende, G., Kollipara, S., Sekar, V., & Saha, R. (2008). UV-spectrophotometric determination of imatinib mesylate and its application in solubility studies. *Pharmazie*, *63*(9), 641-645. https://doi.org/10.1691/ph.2008.8094

Castillo-Cabrera, G. X., Pliego-Cerdán, C. I., Méndez, E., & Espinoza-Montero, P. J. (2023). Step-by-step guide for electrochemical generation of highly oxidizing reactive species on BDD for beginners. *Frontiers in Chemistry*, *11*. https://doi.org/10.3389/fchem.2023.1298630

Domingo-Echaburu, S., Lopez de Torre-Querejazu, A., Valcárcel, Y., Orive, G., & Lertxundi, U. (2022). Hazardous drugs (NIOSH's list-group 1) in healthcare settings: Also a hazard for the environment? *Science of the Total Environment*, *817*, 152954. https://doi.org/10.1016/j.scitotenv.2022.152954

Espinoza-Montero, P. J., Vargas, R., Alulema-Pullupaxi, P., & Fernández, L. (2022). Photoelectrocatalysis: Principles and Applications. En *Advanced Oxidation Processes for Wastewater Treatment* (pp. 53-68). CRC Press. https://doi.org/10.1201/9781003165958-5

Global Petrol Prices. (2024). Ecuador electricity prices.

Gondi, R., Kavitha, S., Yukesh Kannah, R., Parthiba Karthikeyan, O., Kumar, G., Kumar Tyagi, V., & Rajesh Banu, J. (2022). Algal-based system for removal of emerging pollutants from wastewater: A review. *Bioresource Technology*, *344*, 126245. https://doi.org/10.1016/J.BIORTECH.2021.126245

Jerczynski, K., Lipinska, M., Raj, W., Šlouf, M., Halagan, K., Kozanecki, M., Grobelny, J., Matyjaszewski, K., & Pietrasik, J. (2022). Effect of hybrid TiO2 nanoparticles with controlled morphology on rheological properties of poly(styrene-co-acrylonitrile) nanocomposites. *Materials Today Chemistry*, *26*, 101189. https://doi.org/10.1016/j.mtchem.2022.101189

Kayani, Z. N., Abid, H. A., Nazli, H., Shahid, A., Riaz, S., & Naseem, S. (2023). Mg doped TiO2 thin films: Optical, dielectric, photocatalytic, magnetic and antibacterial studies. *Materials Science and Engineering: B*, *297*, 116674. https://doi.org/10.1016/J.MSEB.2023.116674

Klein-Rodewald, T., Micklich, K., Sanz-Moreno, A., Tost, M., Calzada-Wack, J., Adler, T., Klaften, M., Sabrautzki, S., Aigner, B., Kraiger, M., Gailus-Durner, V., Fuchs, H., Aguilar Pimentel, J. A., Becker, L., Garrett, L., Hölter, S. M., Prehn, C., Rácz, I., Rozman, J., & Rathkolb, B. (2022). New C3H Kit N824K/WT cancer mouse model develops late-onset malignant mammary tumors with high penetrance. *Scientific Reports*, *12*(1). https://doi.org/10.1038/s41598-022-23218-5

UNIVERSIDAD TÉCNICA DE MANABÍ
Fundada en 1952

BASES DE LA CIENCIA
REVISTA CIENTÍFICA
FACULTAD DE CIENCIAS BÁSICAS
Portoviejo - Manabí - Ecuador

Mazierski, P., Białk-Bielińska, A., Siedlecka, E., Zaleska-Medynska, A., & Pieczyńska, A. (2023). Role of operating parameters in photoelectrocatalytic degradation of anticancer drugs: Ifosfamide, 5-fluorouracil and imatinib using CdS/TiO2. *Journal of Water Process Engineering*, *51*, 103460. https://doi.org/10.1016/j.jwpe.2022.103460

Mishra, R. K., Mentha, S. S., Misra, Y., & Dwivedi, N. (2023). Emerging pollutants of severe environmental concern in water and wastewater: A comprehensive review on current developments and future research. *Water-Energy Nexus*, *6*, 74-95. https://doi.org/10.1016/j.wen.2023.08.002

Naraginti, S., Yu, Y. Y., Fang, Z., & Yong, Y. C. (2019). Visible light degradation of macrolide antibiotic azithromycin by novel ZrO2/Ag@TiO2 nanorod composite: Transformation pathways and toxicity evaluation. *Process Safety and Environmental Protection*, *125*, 39-49. https://doi.org/10.1016/J.PSEP.2019.02.031

Novak, M., Baebler, Š., Žegura, B., Rotter, A., Gajski, G., Gerić, M., Garaj-Vrhovac, V., Bakos, K., Csenki, Z., Kovács, R., Horváth, Á., Gazsi, G., & Filipič, M. (2021). Deregulation of whole-transcriptome gene expression in zebrafish (Danio rerio) after chronic exposure to low doses of imatinib mesylate in a complete life cycle study. *Chemosphere*, *263*. https://doi.org/10.1016/j.chemosphere.2020.128097

Novak, M., Žegura, B., Nunić, J., Gajski, G., Gerić, M., Garaj-Vrhovac, V., & Filipič, M. (2017). Assessment of the genotoxicity of the tyrosine kinase inhibitor imatinib mesylate in cultured fish and human cells. *Mutation Research - Genetic Toxicology and Environmental Mutagenesis*, *814*, 14-21. https://doi.org/10.1016/j.mrgentox.2016.12.002

Quilumbaquin, W., Castillo-Cabrera, G. X., Borrero-González, L. J., & Espinoza-Montero, P. J. (2024). Protocol for the preparation of TiO2-modified boron-doped diamond photoelectrode via electrophoretic deposition and its photoelectrochemical study. *STAR Protocols*, *5*(3). https://doi.org/10.1016/j.xpro.2024.103259

Quilumbaquin, W., Castillo-Cabrera, G. X., Borrero-González, L. J., Mora, J. R., Valle, V., Debut, A., Loor-Urgilés, L. D., & Espinoza-Montero, P. J. (2024). Photoelectrocatalytic degradation of high-density polyethylene microplastics on TiO2-modified boron-doped diamond photoanode. *iScience*, *27*(3). https://doi.org/10.1016/j.isci.2024.109192

Rycewicz, M., Nosek, A., Shin, D. H., Ficek, M., Buijnsters, J. G., & Bogdanowicz, R. (2022). The effect of boron concentration on the electrical, morphological and optical properties of boron-doped nanocrystalline diamond sheets: Tuning the diamond-on-graphene vertical junction. *Diamond and Related Materials*, *128*, 109225. https://doi.org/10.1016/J.DIAMOND.2022.109225

Serna Siatova, J. C., & Cárdenas Losada, L. Á. (2018). Eventos adversos y problemas relacionados con imatinib reportados [Trabajo de grado, Universidad de Ciencias Aplicadas y Ambientales (UDCA), Facultad de Ciencias de la Salud, Química Farmacéutica, Bogotá].

Sigcha-Pallo, C., Peralta-Hernández, J. M., Alulema-Pullupaxi, P., Carrera, P., Fernández, L., Pozo, P., & Espinoza-Montero, P. J. (2022). Photoelectrocatalytic degradation of diclofenac with a boron-doped diamond electrode modified with titanium dioxide as a photoanode. *Environmental Research*, *212*. https://doi.org/10.1016/j.envres.2022.113362

Sultana, M., Karmakar, S., & Haque, A. (2025). N- and P-type doping of diamonds: A review. *Materials Science in Semiconductor Processing*, *186*, 109024. https://doi.org/10.1016/J.MSSP.2024.109024

Terashima, C., Hishinuma, N., R. Roy, Sugiyama, Y., Latthe, S. S., Nakata, K., Kondo, T., Yuasa, M., & Fujishima, A. (2016). Charge Separation in TiO2/BDD Heterojunction Thin Film for Enhanced Photoelectrochemical Performance. *ACS Applied Materials & Interfaces*, *8*(3), 1583-1588. https://doi.org/10.1021/acsami.5b10993

Vasilachi, I. C., Asiminicesei, D. M., Fertu, D. I., & Gavrilescu, M. (2021). Occurrence and fate of emerging pollutants in water environment and options for their removal. *Water*, *13*(2), 181. https://doi.org/10.3390/w13020181

Wei, L., Guo, Z., & Jia, X. (2021). Probing Photocorrosion Mechanism of CdS Films and Enhancing Photoelectrocatalytic Activity via Cocatalyst. *Catalysis Letters*, *151*(1), 56-66. https://doi.org/10.1007/s10562-020-03275-z

Xie, J., Zhang, C., & Waite, T. D. (2022). Hydroxyl radicals in anodic oxidation systems: generation, identification and quantification. *Water Research*, *217*, 118425. https://doi.org/10.1016/j.watres.2022.118425

Yang, W., Zhou, M., Oturan, N., Li, Y., & Oturan, M. A. (2019). Electrocatalytic destruction of pharmaceutical imatinib by electro-Fenton process with graphene-based cathode. *Electrochimica Acta*, *305*, 285-294. https://doi.org/10.1016/j.electacta.2019.03.067

Zhu, K., Chen, Y., Wang, Y., Feng, M., & Zhao, Y. (2022). Progress of solution-processed metal oxides as charge transport layers towards efficient and stable perovskite solar cells and modules. *Materials Today Nano*, *20*, 100252. https://doi.org/10.1016/J.MTNANO.2022.100252

8. Contributions from authors

Author	Contribution
Steven Mateo Vélez Zambrano	Data curation, Formal analysis, Investigation, Methodology, Writing- original draft, Writing - review & editing.
G. Xavier Castillo-Cabrera	Data curation, Formal analysis, Investigation, Methodology, Writing - review & editing.
Gustavo Altamirano-Briones	Conceptualization, Funding acquisition, Investigation, Methodology, Resources, Supervision, Validation, Visualization, Writing - original draft, Writing - review & editing.
Patricio Javier Espinoza-Montero	Conceptualization, Data curation, Funding acquisition, Investigation, Methodology, Project administration, Resources, Supervision, Validation, Visualization, Writing - original draft, Writing - review & editing.

UNIVERSIDAD TÉCNICA DE MANABÍ
Fundada en 1952

BASES DE LA CIENCIA
REVISTA CIENTÍFICA
FACULTAD DE CIENCIAS BÁSICAS
Portoviejo - Manabí - Ecuador

9. Supplementary material

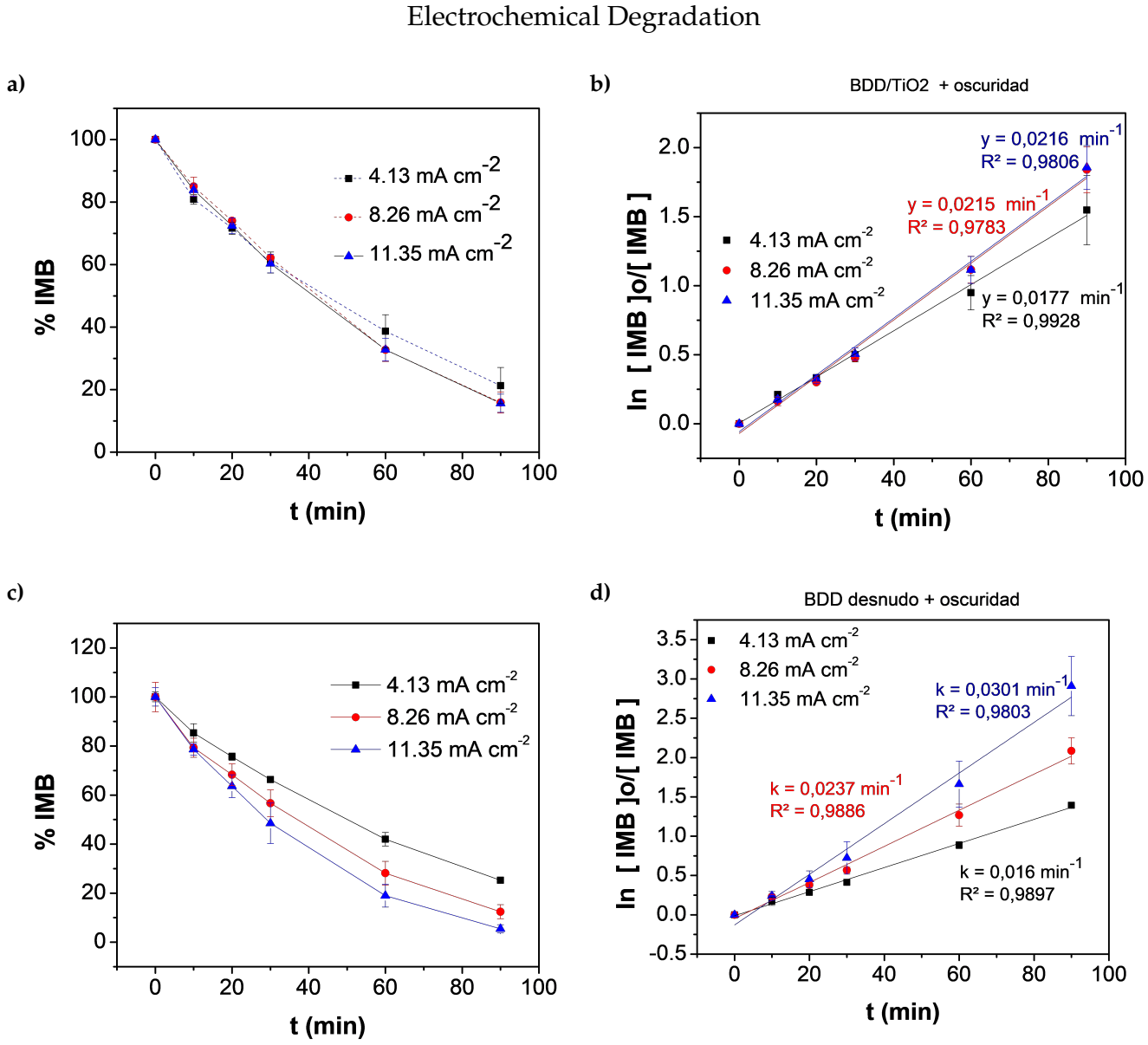

Figure S1. a) Degradation efficiency of IMB during 90-min EO process using a BDD/TiO_2 photoanode at different current densities in 0.1 mol L^{-1} Na_2SO_4. Data are presented as mean ± standard deviation, as detailed in Table S1. b) Pseudo-first-order reaction kinetic analysis of IMB degradation in EO using BDD/TiO_2. c) Degradation efficiency of IMB during 90-min EO process using bare BDD photoanode at different current densities in 0.1 mol L^{-1} Na_2SO_4. Data are presented as mean ± standard deviation, as detailed in Table S1. d) Pseudo-first-order reaction kinetic analysis of IMB degradation in EO using bare BDD.

revista.bdlaciencia@utm.edu.ec | Vol. 10. Núm. 3 (30-43): septiembre-diciembre, 2025 | DOI: 10.33936/revbasdelaciencia.v10i3.7677

Table S1. Mean standard deviation of the percentage of IMB degraded by the photoelectrocatalytic process (PEC) and its kinetic analysis during 90-minute reactions at different current densities applied in 0.1 mol L^{-1} Na_2SO_4, corresponding to Figure 3.

Time (min)	Degradation			Kinetic analysis		
	4.13 mA cm^{-2}	8.26 mA cm^{-2}	11.35 mA cm^{-2}	4.13 mA cm^{-2}	8.26 mA cm^{-2}	11.35 mA cm^{-2}
10	0.91	4.18	1.41	0.00	0.00	0.00
20	4.46	8.41	6.03	0.05	0.07	0.09
30	2.94	7.46	7.70	0.04	0.07	0.12
60	1.95	6.36	8.14	0.04	0.08	0.16
90	11.94	7.13	8.19	0.23	0.21	0.32
Mean standard deviation	4.44	6.71	6.29	0.07	0.09	0.14

Table S2. Mean standard deviation of the percentage of IMB degraded by the photoanode electrooxidation process (EO-BDD/TiO_2) and its kinetic analysis during 90-minute reactions at different current densities applied in 0.1 mol L^{-1} Na_2SO_4, corresponding to Figure S1.

Time (min)	Degradation			Kinetic analysis		
	4.13 mA cm^{-2}	8.26 mA cm^{-2}	11.35 mA cm^{-2}	4.13 mA cm^{-2}	8.26 mA cm^{-2}	11.35 mA cm^{-2}
10	0.79	10.62	1.64	0.00	0.00	0.00
20	1.44	12.53	3.15	0.02	0.03	0.02
30	2.41	8.29	3.01	0.02	0.01	0.03
60	3.67	6.95	3.27	0.05	0.01	0.04
90	5.31	4.37	2.89	0.12	0.10	0.10
Mean standard deviation	2.72	8.55	2.79	0.04	0.03	0.04

Table S3. Mean standard deviation of the percentage of IMB degraded by the electrooxidation process (EO-BDD) and its kinetic analysis during 90-minute reactions at different current densities applied in 0.1 mol L^{-1} Na_2SO_4, corresponding to Figure S1.

Time (min)	Degradation			Kinetic analysis		
	4.13 mA cm^{-2}	8.26 mA cm^{-2}	11.35 mA cm^{-2}	4.13 mA cm^{-2}	8.26 mA cm^{-2}	11.35 mA cm^{-2}
10	0.00	0.00	0.00	1.99	5.98	3.75
20	0.05	0.02	0.06	3.76	3.87	2.28
30	0.03	0.02	0.11	1.52	4.45	4.66
60	0.01	0.04	0.21	0.79	5.42	8.28
90	0.04	0.14	0.29	2.74	4.81	4.66
Mean standard deviation	0.03	0.04	0.13	2.16	4.91	4.73

UNIVERSIDAD TÉCNICA DE MANABÍ
Fundada en 1952

BASES DE LA CIENCIA
REVISTA CIENTÍFICA
FACULTAD DE CIENCIAS BÁSICAS
Portoviejo - Manabí - Ecuador

Table S4. Mean standard deviation of the values obtained by chemical oxygen demand for the three degradation processes during 90 minutes, at a current density of 8.26 mA cm^{-2}, corresponding to Figure 4.

	PEC	EO-BDD-TiO_2	EO-BDD
Time (min)	**8.26 mA cm^{-2}**	**8.26 mA cm^{-2}**	**8.26 mA cm^{-2}**
10	0.65613	0.56569	4.17193
20	1.98756	1.59099	2.72236
30	2.52937	1.69706	4.34871
60	0.44252	1.06066	5.16188
90	0.71	1.27279	3.81838
Mean standard deviation	1.27	1.24	4.04

revista.bdlaciencia@utm.edu.ec | Vol. 10. Núm. 3 (30-43): septiembre-diciembre, 2025 | DOI: 10.33936/revbasdelaciencia.v10i3.7677